

Engineered Cationic Antimicrobial Peptides Containing Cholesterol Interacting Motifs to Target Viral Envelopes

Mary L Hasek^{1,2}, Jonathan D Steckbeck^{1,3}, Berthony Deslouches^{1,3}, Jodi K Craigo^{1,3*} and Ronald C Montelaro^{1,3}

¹Center for Vaccine Research, University of Pittsburgh, Pittsburgh, Pennsylvania, United States of America

²Department of Infectious Diseases and Microbiology, University of Pittsburgh Graduate School of Public Health, Pittsburgh, Pennsylvania, United States of America

³Department of Microbiology and Molecular Genetics, University of Pittsburgh School of Medicine, Pittsburgh, Pennsylvania, United States of America

*Corresponding author: Jodi K Craigo, Center for Vaccine Research, University of Pittsburgh, Pittsburgh, Pennsylvania, United States of America, Tel: 412-648-8874; Fax: 412-624-4440; E-mail: craigoj@pitt.edu

Received date: March 31, 2017, Accepted date: April 18, 2017, Published date: April 30, 2017

Copyright: © 2017 Hasek ML, et al. This is an open-access article distributed under the terms of the Creative Commons Attribution License, which permits unrestricted use, distribution, and reproduction in any medium, provided the original author and source are credited.

Abstract

In recent decades, efforts have been made to rationally design antimicrobial peptides (AMPs) for use as alternative antimicrobial therapeutics. The *de novo* engineered cationic antimicrobial peptide (eCAP) WLBU2 is a 24-residue peptide composed of arginine, tryptophan, and valine computationally sequenced to form an optimized amphipathic helix. Antimicrobial activity of WLBU2 is predicted to transpire through peptide interaction with lipid membranes leading to bilayer disruption. Antibacterial activity of WLBU2 has been demonstrated against a wide-range of antibiotic resistant Gram-positive and Gram-negative bacteria. Natural antimicrobial peptides have been shown to inactivate enveloped viruses, albeit at higher peptide concentrations than required for bacterial killing. While viral envelopes do not have the same negative surface charge presumed to be the basis for antibacterial activity of WLBU2, most mammalian virus membranes are enriched for cholesterol relative to host cells. Based on this structural feature, WLBU2 was modified by addition of cholesterol recognition amino acid consensus (CRAC) motifs to increase antiviral activity against enveloped mammalian viruses. The CRAC-modified WLBU2 peptides were tested against human immunodeficiency virus (HIV), influenza A, and dengue virus (DENV) to assess antiviral activity against viruses with markedly different levels of surface lipid exposure and against mammalian cells to assess potential cytotoxicity. Antiviral activity was enhanced by the CRAC motif and demonstrated the highest efficacy against DENV and lowest against HIV, inverse to the level of surface membrane exposure. These studies reveal for the first time an unexpected range of engineered peptide activity against a broad group of different target viruses with vastly different membrane compositions and indicate the ability of CRAC motif modification to enhance antiviral activity.

Keywords: Antimicrobial peptide; Cholesterol; CRAC motif; Viral envelope

Introduction

Viral infectious diseases remain a threat worldwide despite significant medical advances. Few approved antiviral treatments exist and most antiviral drugs are limited to a single type of viral pathogen [1]. In recent decades, there has been an increasing interest in the development of antimicrobial peptides (AMPs) as potential novel therapeutic agents against bacteria, viruses, and fungi [2-4]. Naturally occurring AMPs are produced by animals and plants as important components of the innate immune response [5,6] and have evolved to respond to properties of microbes that are not dependent on pathogen metabolic activity [7]. Most naturally occurring AMPs are commonly made of fewer than 100 amino acids (32 average), have a net positive charge, and form an amphipathic structure [8,9]. Naturally occurring AMPs have been selected through evolutionary pressures as anti-infective agents that have activity against specific pathogens in specific physiological environments [6,10]. To date, however, these natural AMPs have proven ineffective in clinical human applications, perhaps due to this specificity of activity to certain biological environments and target pathogens [11-13].

Engineered cationic antimicrobial peptides (eCAPs) have been rationally designed *de novo* to increase the range of activity against

different pathogens in various biological environments [14,15]. The eCAP WLBU2, a 24-mer composed of only arginine, valine, and tryptophan to form an optimized amphipathic helix, displays antimicrobial activity *in vitro* against a broad range of Gram-positive and Gram-negative bacteria including multi- and pan-drug resistant strains. [16-18]. In addition, WLBU2 has proven effective *in vivo* in the treatment of systemic bacterial infections in mouse models [19]. For viral infections, *in vitro* studies using several AMPs, both naturally occurring and engineered, have indicated antiviral activity against several mammalian viruses, although effective concentrations are higher than those observed against bacteria [20-23]. Mechanisms of antiviral activity for a single peptide can apparently differ based on the target virus, as observed with the human cathelicidin LL-37 against human immunodeficiency virus (HIV) [24-26]. Preliminary experiments using WLBU2 have indicated antiviral activity against clinical isolates of herpesvirus [27]. A peptide with both anti-bacterial and anti-viral activity could be of great therapeutic potential. However, the required higher concentrations of peptides for anti-viral efficacy limit its potential for clinical use. In order to increase the antiviral activity of engineered peptides, properties of viral envelopes shared among various families of viruses could be exploited in order to create membrane disruptive peptides that preferentially target viral envelopes [28].

Specifically targeting viral envelopes is difficult because the phospholipid profiles of viral and host cellular lipid membranes are

similar [29]. Viral envelope lipids lack the high concentration of negative charge that is the basis of AMP interaction with and disruption of bacterial membranes [30]. However, studies of viral envelopes identified a higher cholesterol-to-phospholipid (Chol/Phos) ratio compared to the host membranes from which they are derived [31-34]. This cholesterol enrichment has also been shown to be necessary for virus infectivity [35-37]. Exploiting cholesterol enrichment would allow for higher viral efficacy AMPs at lower concentrations, more similar to concentrations used for anti-bacterial activity while also reducing the cytotoxicity to host cells. An amino acid sequence called the cholesterol recognition amino acid consensus sequence (CRAC) motif directs proteins to cholesterol-rich membranes [38], representing a plausible targeting strategy for enveloped virus inactivation. The CRAC motif is a flexible sequence of 5 to 13 amino acids long that directs proteins to cholesterol rich regions of membranes. The consensus sequence is L/V-X (1-5)-Y-X (1-5) -R/K, in which X (1-5) represents one to five residues of any amino acid. This motif is thought to function by interacting directly with a cholesterol molecule, where the central tyrosine stabilizes interactions by forming H-bonds [39]. Proper CRAC function relies on structural flexibility of the motif to allow for stable and specific interaction with cholesterol [40].

Thus the addition of the CRAC motif to WLBU2 could potentially direct peptides to cholesterol rich membranes such as the viral envelope. Since antibacterial activity of WLBU2 is presumed to be based on membrane disruption, we theorized that CRAC motif containing peptides could display antiviral activity based on viral envelope disruption, where viruses with greater surface lipid exposure would be more sensitive to peptide treatment. For this study, a reference panel of three mammalian enveloped viruses was chosen based on markedly different levels of membrane protein content and surface lipid exposure: human immunodeficiency virus (HIV), influenza A, and dengue virus (DENV). We hypothesized that accessibility to the lipid membrane affects antiviral activity of membrane disruptive peptides based on the ability of the peptide to form stable and specific interactions with viral envelopes. The surface of the HIV virion is sparsely populated with about 7-11 copies of the Env trimer allowing for high lipid exposure [41] and has been shown to have a high cholesterol content as compared to mammalian cells [42]. The influenza A virion surface is coated with three membrane proteins: hemagglutinin, neuraminidase, and the M2 matrix protein [43]. While there is a much higher membrane protein content for influenza A as compared to HIV, access to the lipid surface is still possible, especially by small molecules [44]. Dengue virus (DENV) has the lowest lipid exposure of this panel, as the viral envelope is enclosed within a proteinaceous, icosahedral shell of E protein dimers [45-47]. Analysis of antiviral activity of CRAC motif containing peptides against this panel of viruses indicates whether peptide activity is dependent upon accessibility of the viral envelope lipids.

In the current study we test the hypothesis that the addition of CRAC motif sequences to WLBU2 would increase eCAP activity against lipid enveloped viruses and that the level of antiviral activity would be directly related to the extent of lipid exposure at the virion surface, i.e., viruses with greater lipid exposure would be the most susceptible to eCAP inactivation. The experimental results reveal otherwise.

Materials and Methods

Modeling of CRAC-WLBU2 peptides

The peptide modeling program PEP-FOLD (<http://bioserv.rpbs.univ-paris-diderot.fr/PEP-FOLD/>) was used to predict the conformational structure of CRAC motif-containing WLBU2 peptides. Sequences were analyzed on a short simulation and models were sorted by sOPEP, which clusters models with simplified side chains based on similar energy states [48]. PEP-FOLD predicts peptide conformations based on the specific amino acid sequence using coarse-grain simulation to calculate interactions between four amino acids at a time [49]. Models generated in PEP-FOLD are sorted into clusters based on structural similarity. All models that were analyzed were representative of a single model cluster. Models generated from PEP-FOLD were then examined using PyMol molecular visualization software version 0.99 (<http://www.pymol.org/>). Similarly, helical wheel projections and hydrophobicity predictions were created by HeliQuest (<http://heliquest.ipmc.cnrs.fr/>). Helical wheel projections were created using the α -helix setting to analyze the full amino acid sequence. This program then analyzes the physicochemical properties of the peptide based on its amino acid sequence and the forced helical conformation [50].

Peptide synthesis

Amino acid sequences of the desired peptides (WLBU2 and CRAC-modified versions) were produced by the University of Pittsburgh Peptide Synthesis Core following previously reported synthesis, purification, and quality control procedures optimized for WLBU2 production [51]. The same peptides were also produced commercially by Genscript (Piscataway, NJ) using similar production methods. All peptide preparations were purified by HPLC to at least 95% purity. Concentrations of peptide dissolved in sterile water were determined by a standard ninhydrin assay as previously reported [51]. Concentrations were confirmed using spectrophotometric methods by A260/A280 determination on a NanoDrop 1000 spectrophotometer (NanoDrop, Wilmington, DE).

Circular dichroism spectroscopy

Measurements were taken at a 40 μ M concentration of each peptide in the following solvent environments: deionized water, 6 mM sodium dodecyl sulfate (SDS), 30 mM SDS, and 30% tetrafluoroethylene (TFE). Circular dichroism (CD) measurements were taken with a Jasco spectrometer (Aviv Instruments, Lakewood, NJ) at room temperature with a 1 mm path length over 185 nm to 260 nm with machine units as output for five scans per sample. The mean residue ellipticities ($[\Theta]/1,000 \times [(\text{degree} \times \text{square centimeters})/\text{decimole}]$) were calculated of the averaged five scans using Dichroweb (<http://dichroweb.cryst.bbk.ac.uk/>) [52]. These data were analyzed using the CDSSTR method [53-55] with SP175 as the reference data set [56].

Cell propagation

The following cell lines were propagated in Dulbecco's Modified Eagle Medium (DMEM; Life Technologies, Grand Island, NY) containing 10% fetal bovine serum (FBS) and 1% L-glutamine (Corning, Manassas, VA): MDCK (ATCC CCL-34), MRC-5 (ATCC CCL-171), HEK293T/17 (ATCC ACS-4500), VeroE6 (ATCC CRL-1586), and TZM-bl (Cat No: 8129, NIH AIDS Research and Reference Reagent Program, Germantown MD) cells. Cultured cells

were passaged by treatment with 0.05% Trypsin/0.53 mM EDTA in HBSS (Corning, Manassas, VA) for 10-15 minutes before transferring a subset of cells to a new flask with fresh complete media.

Virus pretreatment assays

To assay HIV inactivation by test eCAPs, a viral infection neutralization assay was carried out on TZM-bl cells in 96-well flat bottom plates to measure production of luciferase under control of the HIV-1 promoter [57]. Cells were plated at a concentration of 2.5×10^4 cells/well and allowed to adhere at 37°C/5% CO₂ for 7 h. HIV strain 89.6 was diluted so as to produce approximately 3×10^4 RLU/well in untreated control wells. Peptide dilutions were prepared in a 96-well U-bottom plate by 2-fold serial dilutions starting at 100 µM down to 0.78 µM in DMEM containing 10% FBS. Equal volumes of virus stock were added to each well of peptide and incubated together at 37°C/5% CO₂ for 1 h. Virus-peptide mixtures were then diluted 5-fold and plated on adhered TZM-bl cells for 1 h, at which time the supernatant was removed and replaced with fresh complete media. Plates were incubated for 48 h, cells were then lysed with 50 µL of cell culture lysis reagent (Promega, Madison WI), and luciferase activity was measured using the luciferase assay system according to the manufacturer's instructions (Promega, Madison WI) using an Orion Microplate Luminometer (Berthold, Oak Ridge TN).

To assay influenza A inactivation by test eCAPs, a plaque assay was carried out on MDCK cells [58] using virus that had been pre-incubated with different concentrations of test peptides. Influenza strain PR8 was diluted to a final concentration of 160 pfu/ml then mixed with an equal volume of prepared dilutions of peptide. Peptide had been diluted by 2-fold serial dilution using DMEM containing 0.2% BSA in 1.5 mL Eppendorf tubes starting at 100 µM down to 0.78 µM. Peptide-virus mixtures were incubated at 37°C/5% CO₂ for 1 h. MDCK cells between passages 3 and 10 plated in 6-well plates were grown to 90-100% confluence and washed twice with serum-free media then exposed to pre-incubated virus-peptide mixtures for 45 minutes in duplicate. Virus and peptide were removed and replaced with plaquing media containing DMEM, 10% FBS, 2.5 µg/mL TPCK-treated Trypsin, and 0.4% agarose. Infected and treated cells were then grown at 37°C/5% CO₂ for 5 days before being stained with 35% EtOH/0.25% crystal violet overnight at 4°C. Stain and agarose plugs were removed and plaques were counted by eye using a light box.

To assay DENV inactivation by test eCAPs, a plaque assay was carried out on VeroE6 cells [59] using serotype 2 virus that had been pre-incubated with various concentrations of peptide. Virus was diluted to approximately 1200 pfu/ml and mixed with an equal volume of prepared dilutions of peptide. Peptide had been diluted by 2-fold serial dilution using MEM containing penicillin/streptomycin, and Fungizone (Life Technologies, Grand Island NY) in a 96-well plate starting at 50 µM to 1.5625 µM. Peptide-virus mixtures were incubated at 37°C/5% CO₂ for 1 h. VeroE6 cells between passages 25 and 42 plated in 24-well plates were grown to 90-100% confluence over 48 h and then exposed to pre-incubated virus-peptide mixtures for 1 h in duplicate. Virus and peptide were removed and replaced with semi-solid media containing 3% carboxymethylcellulose (CMC), MEM, 10% FBS, 1% penicillin/streptomycin (Corning, Manassas, VA), and 1% Fungizone. Infected and treated cells were then grown at 37°C/5% CO₂ for 6 days before fixing and staining. Semi-solid medium was removed from cells before addition of formalin and cells were then allowed to incubate at room temperature for 1 h. Formalin was removed, the cells were washed, and then crystal violet was added. Plates were incubated

for 1 h at room temperature and washed again before plaques were counted by eye using a light box. All inactivation assays were performed at least three times.

Vero cell pretreatment assay

To assay whether pretreating Vero E6 cells with test eCAPs before infection with DENV serotype 2, a foci forming unit (FFU) assay was carried out. Vero E6 cells between passage 27 and 33 plated in 12-well plates were grown to 90-100% confluence over 24 h and then exposed to various concentrations of peptide in duplicate. Peptide dilutions were made in serum-free DMEM and ranged in concentration from 25 µM to 0.39 µM. Peptides were removed from cells after 1 h treatment at 37°C/5% CO₂ and cells were washed twice with room temperature PBS. DENV serotype 2 was diluted to concentration of 100 FFU/mL in DMEM and cells were infected with 0.3 mL/well of virus. Cells were incubated with virus for 1 h at 37°C/5% CO₂ before removal virus. Cells were washed twice with room temperature PBS and overlaid with semi-solid media containing Optimem (Gibco, Grand Island, NY), 0.8% methyl cellulose, 3% FBS, 1% L-glutamine, and 1% penicillin/streptomycin. Cells were incubated at 37°C/5% CO₂ for 5 days before developing plates. Semi-solid media was removed by aspiration and cells were washed twice with room temperature PBS before being fixed in 1:1 methanol:acetone for 30 min at room temperature. Cells were blocked for 1 h at room temperature in PBS containing 3% FBS. Anti-Dengue Virus Complex Antibody, clone D3-2H2-9-21 (EMD Millipore, Darmstadt, Germany), diluted 1:400 was added to cells for overnight incubation. Cells were washed three times with room temperature PBS before addition of Goat anti-Mouse IgG Secondary Antibody, HRP conjugate (ThermoFisher, Waltham, MA). After 1 h room temperature incubation, cells were washed three times with PBS before addition of TrueBlue Peroxidase substrate (KPL, Gaithersburg, Maryland) for 20 min at room temperature. Cells were washed once with dH₂O and allowed to dry overnight before counting foci. Inactivation was calculated as the number of foci found in pretreatment wells as compared to control wells that had been treated with DMEM alone.

MTS Assay of cytotoxicity

Cytotoxicity measurements were taken on selected transformed and non-transformed cells using a tetrazolium-based colorimetric MTS assay, a one-step variation of the classic MTT assay [60,61]. The MTS assay measures cell viability by detecting metabolically active cells that reduce MTS to a colored formazan reagent [62]. Cells were plated in 96-well plates and allowed to grow to 90-100% confluence. Peptides starting at 50 µM were serially diluted by two-fold in a 96-well U-bottom plate and incubated at 37°C/5% CO₂ for 1 h. Cells were then treated with peptides for 1 h, at which time the peptide-containing supernatant was removed and replaced with fresh complete media. Cells were then allowed to recover at 37°C/5% CO₂ for 4 h before performing an MTS assay. This assay was carried out using the CellTiter 96 Aqueous One Solution Cell Proliferation Assay following the manufacturer's protocol (Promega, Madison, WI). Briefly, MTS reagent was added to cells, and then incubated at 37°C/5% CO₂ for 2 h before spectrophotometric readings were taken at 490 nm on a SpectraMax 340PC384 Absorbance Microplate Reader (Molecular Devices, Sunnyvale, CA). Cytotoxicity assays were carried out at least three times against each cell line.

Human red blood cell lysis assay

A modified version of the RBC lysis assay described by Deslouches et al. [16] was performed samples of heparinized human blood purchased from BioChemed (Winchester, VA <http://www.biochemed.com/human-biological-products.php>); University of Pittsburgh IRB approved exempt status for these specimens. Peptide dilutions ranging in concentration from 100 μM to 0.78 μM were prepared in duplicate in tissue culture-treated round bottom 96-well plates. Peptides were incubated at 37°C/5% CO₂ for 1 h to mimic viral inactivation assays before an equal volume of whole blood was added to each well (1:2 dilution). To produce a standard curve for analysis, 0 to 50 μl of 1:2 diluted whole blood was added to dH₂O to a final volume of 500 μl and incubated for 1 h along with peptide-whole blood mixtures at 37°C/5% CO₂. These treated red blood cells suspensions were then centrifuged at 600 x g for 5 minutes to pellet intact RBCs. In a 96-well flat bottom plate, supernatant from each peptide-whole blood mixture was diluted 10-fold in sterile dH₂O. Absorbance readings were taken at 570 nm on a SpectraMax 340PC384 Absorbance Microplate Reader (Molecular Devices, Sunnyvale, CA). Hemolysis assays were carried out least three times.

Isolation of human peripheral blood monocytes

PBMCs were isolated from healthy samples of heparinized human blood purchased from Bio Chemed (Winchester, VA <http://www.biochemed.com/human-biological-products.php>); University of Pittsburgh IRB approved exempt status for these specimens. PBMC were isolated by Ficoll gradient centrifugation using Lymphocyte Separation Media (MP Biomedicals, Santa Anna, CA). Collected PBMC were washed with PBS at least twice, and treated with ACK lysis buffer (Gibco, Grand Island, NY) as needed to remove erythrocytes. Following isolation, PBMC were incubated for 48 h at 37°C/5% CO₂ in DMEM/20% FBS before use in further experiments.

Flow cytometric analysis of cell viability

PBMC were exposed to peptide dilutions in DMEM/10% FBS that had been pre-incubated for 1 h at 37°C/5% CO₂. After one hour, peptide supernatants were removed by centrifugation, washed once, and resuspended in PBS. Cells were immediately stained using LIVE/DEAD Fixable Blue Dead Cell Stain Kit (Invitrogen, Grand Island, NY) following the manufacturer protocol. Cells were then fixed using 2%

methanol-free formaldehyde by incubation at room temperature for 15 minutes. Cells were washed once more with PBS before analysis on a BD LSRII (BD, Franklin Lakes, NJ). Cell viability assays were carried out at least three times.

Statistical analysis

Statistical analysis of the data from repeat experiments was performed using GraphPad Prism 6 (La Jolla, CA). EC₅₀ and CC₅₀ values were calculated using the nonlinear fit of log [agonist] vs. response. Ordinary one way ANOVA using multiple comparisons and Tukey's test was used to determine the statistical significance between peptides in each treatment.

Results

CRAC motif design and predictive modeling of N- and C-terminal CRAC motif additions to WLBU2

Following the consensus sequence (L/V-X (1-5)-Y-X (1-5)-K/R), CRAC motifs were designed for incorporation into WLBU2 in an attempt to increase cholesterol specificity. Two CRAC motifs were used: LWYIK, derived from HIV gp41 [40,63,64], and VWYVK, a synthetically designed CRAC motif created to minimize amino acid differences between WLBU2 and the CRAC sequence. CRAC motif function has been shown to be optimized in a context where the CRAC sequences are able to assume a flexible, unordered structure [40]. Modeling was carried out using readily-accessible programs to examine the predicted effect of CRAC motif influence on WLBU2 structure as a basis to determine the optimal location for this modification in the peptide sequence. These structural modeling studies employed PEP-FOLD modeling software, which has been optimized to predict secondary structure of short amino acid sequences based on a coarse grain, multiple simulation analysis using a structural alphabet for reference [48,49]. Each CRAC motif, LWYIK and VWYVK, was added to either the C- or N-terminus of the WLBU2 sequence and modeled using PEP-FOLD. According to modeling predictions, addition of the CRAC motif to the C-terminus of WLBU2 resulted in a largely helical structure maintained throughout the peptide, including the C-terminal CRAC motif (Figure 1A).

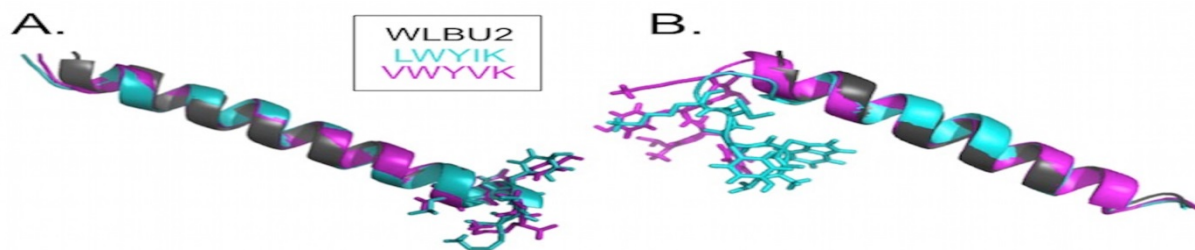


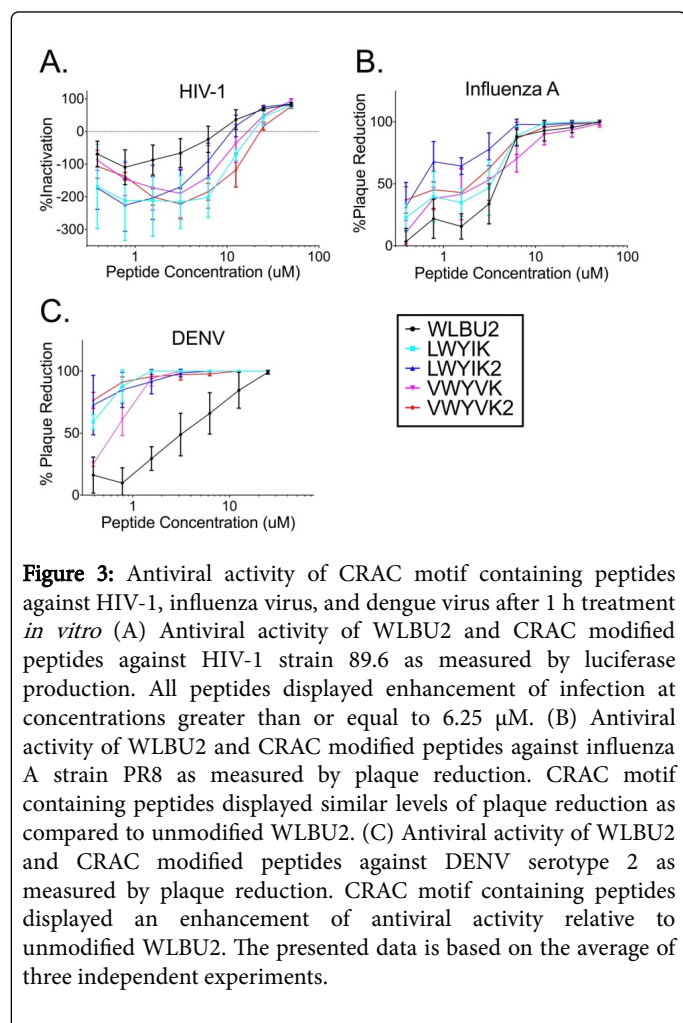
Figure 1: Structural models of WLBU2 containing one CRAC motif. Models of WLBU2 containing each CRAC motif on either (A) the C-terminus or (B) the N-terminus. WLBU2 is represented by gray models, LWYIK containing peptides are represented in blue, and VWYVK containing peptides are represented in pink.

Because PEP-FOLD models the C-terminal CRAC motif as helical, the structure is predicted to lack the flexibility necessary for proper CRAC motif function [39]. According to modeling predictions for N-

terminal CRAC peptides, the helix of WLBU2 was undisturbed while the N-terminal CRAC motifs assume an unstructured conformation

μM to $0.39 \mu\text{M}$) of each of the peptides, and the level of infectious virus was assayed on TZM-bl cells (Figure 3A). Percent inactivation of HIV was calculated based on comparison of luciferase production to untreated HIV controls. For each of the peptides tested, viral inactivation was observed only at the highest peptide concentrations, 50 and $25 \mu\text{M}$. Unexpectedly, treatment of HIV with CRAC motif containing peptides at concentrations below $25 \mu\text{M}$ resulted in apparent enhancement of HIV infection. For example, at $6.25 \mu\text{M}$, CRAC motif containing peptides enhanced infection 1-to 2-fold over untreated controls. Interestingly, the parental WLBU2 peptide displayed inactivation and enhancement properties similar to the CRAC-modified peptides, indicating that the observed functional properties were not the direct result of the CRAC motif.

Influenza A virions has intermediate membrane protein contents, with a moderate surface lipid exposure [66]. In order to determine antiviral activity of the CRAC-modified peptides against influenza virus *in vitro*, inactivation by the test peptides was assessed by measuring viral infectivity in a standard plaque assay. Influenza A H1N1 strain PR8 was pretreated with varying concentrations of each of the peptides and then inoculated on MDCK cells (Figure 3B).



Percent plaque reduction was calculated based on comparison to untreated viral controls. The data reveal that all of the CRAC motif containing-peptides have similar activity against influenza as unmodified WLBU2. At concentrations greater than $6.25 \mu\text{M}$, all

peptides reduced plaques by about 90-100%. Even at sub-micromolar concentrations, some peptides retained antiviral activity. At $0.39 \mu\text{M}$, LWYIK2 reduced plaques by about 32%, while VWYVK2 reduced plaques by 37%. However, at the same concentration, WLBU2 has no activity against influenza A, although there was no statistically significant difference in activity between CRAC motif containing peptides and unmodified WLBU2. As summarized in table 3, EC_{50} values indicate that peptides are able to reduce influenza A infectivity at concentrations of approximately 1– $3.5 \mu\text{M}$.

Peptide	Influenza A	DENV
WLBU2	3.5 ± 0.7	3.2 ± 0.9
LWYIK	1.9 ± 0.6	$0.3 \pm 0.1^*$
LWYIK2	0.6 ± 0.2	$0.2 \pm 0.2^*$
VWYVK	2.1 ± 0.6	0.6 ± 0.1
VWYVK2	1.2 ± 0.4	$0.2 \pm 0.1^*$

* $P < 0.05$, as compared to WLBU2

Table 3: Calculated EC_{50} values (μM) against Influenza A virus strain PR8 and DENV serotype 2.

DENV was chosen as a model virus with high membrane protein content and very low lipid surface exposure [45,47]. In order to determine antiviral activity of CRAC-modified peptides against DENV *in vitro*, inactivation was assessed by measuring infectivity in a standard plaque assay. DENV serotype 2 was pretreated with varying concentrations of each of the test peptides and then inoculated on VeroE6 cells (Figure 3C). Percent plaque reduction was calculated based on comparison to untreated controls. All of the test peptides reduced DENV infectivity, and CRAC motif containing peptides outperformed unmodified WLBU2 alone. All the CRAC motif containing peptides displayed almost 100% plaque reduction at concentrations as low as $1.56 \mu\text{M}$. Even at $0.39 \mu\text{M}$, the lowest concentration tested, LWYIK2 and VWYVK2 reduced plaques by 73% and 76%, respectively. CRAC motif containing peptides LWYIK, LWYIK2, and VWYVK2 had statistically significantly greater antiviral activity than unmodified WLBU2 ($P < 0.05$). As summarized in Table 3, EC_{50} values of LWYIK, LWYIK2, and VWYVK2 are about 10-to 20-fold lower than that of WLBU2 alone with 50% reduction of plaques observed at sub-micromolar concentrations. Taken together these data indicate that WLBU2 and CRAC motif containing peptides all reduce infection by DENV serotype 2 *in vitro* and that CRAC motifs significantly improve the efficacy of peptide inactivation of the DENV.

Assessment of anti-DENV activity in cell pretreatment assay using CRAC motif containing peptides

In order to determine whether the anti-DENV activity observed in virus pretreatment assays *in vitro* was due to peptide interaction with cells or with target virus, Vero E6 cells were pretreated with the most active CRAC motif containing peptides LWYIK, LWYIK2, and VWYVK2 for one hour before removal of peptide and infection with DENV serotype 2 and compared to inactivation in virus pretreatment assays (Figure 4). Cells were pretreated with $1.56 \mu\text{M}$ peptide as this was the lowest concentration where 100% inactivation was observed in

virus pretreatment assays. Percent inactivation was calculated based on comparison to cells treated with media containing no peptide. At the tested concentration, pretreatment of cells with CRAC motif containing peptides resulted in less than 50% reduction in DNEV virus infection, whereas at the same concentration in virus pretreatment assays, nearly 100% inactivation is observed. These differences are statistically significant with $P < 0.005$. These data indicate that antiviral activity of the peptide is optimized when present during infection and that peptide interaction with cells can account for some antiviral activity, perhaps by binding to negatively charged cell surface molecules that are known to enhance viral infection.

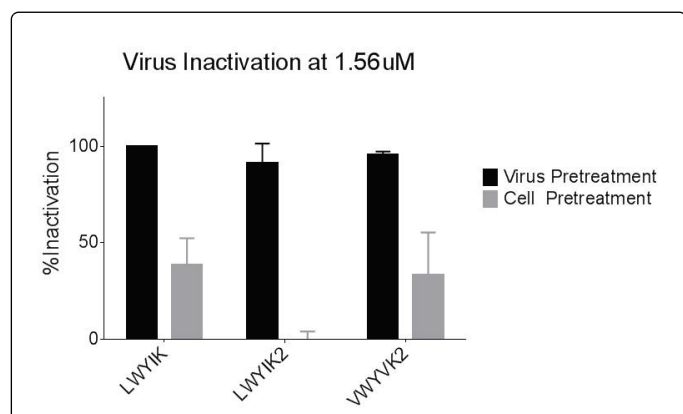


Figure 4: Antiviral activity of CRAC motif containing peptides against DENV serotype 2 in 1 h cell pretreatment assay. Antiviral activity of the best candidate CRAC motif containing peptides was assessed by cell pretreatment assay to determine whether peptide presence during infection is necessary for antiviral activity. VeroE6 cells were pretreated with 1.5625 uM peptide for 1 h before peptide was removed and cells were infected with DENV serotype 2. Infection was measured by standard FFU assay based on two independent experiments each performed in duplicate.

Cell viability assessed by MTS assay against a panel of transformed and non-transformed cells following CRAC motif containing peptide treatment

MTS assays were carried out on a panel of transformed and non-transformed cells to examine the effects of peptide treatment on cell viability to parallel the experiments previously performed by Deslouches et al. [16]. Two transformed cell lines, MDCK and Vero cells, were analyzed as they are the relevant indicator cells used for the influenza A and DENV viral inactivation assays, respectively. The human fetal foreskin fibroblast cell line, MRC-5, was analyzed for a non-transformed cell line [67,68]. Cells were treated with various concentrations of each peptide, and then allowed a four hour recovery period in fresh complete media before cell viability measurements were taken. The cytotoxicity levels are expressed as a percentage of cell viability compared to untreated controls. Figure 5A-5C summarizes the viability of the various cells treated with concentrations of each of the peptides ranging from 50 uM to 0.39 uM. The cytotoxicity levels are expressed as a percentage of cell viability compared to untreated controls.

Peptide	Transformed		Non-transformed
	MDCK	Vero	MRC-5
WLBU2	30.6 ± 4.9	39.6 ± 8.4	31.2 ± 6.7
LWYIK	21.1 ± 2.7	43.5 ± 4.7	21.9 ± 3.5
LWYIK2	20.7 ± 3.7	29.1 ± 4.2	26.5 ± 4.6
VWYVK	23.3 ± 3.0	31.2 ± 2.9	32.4 ± 3.6
VWYVK2	22.0 ± 2.3	33.9 ± 5.0	36.5 ± 6.5

Table 4: Calculated CC_{50} values (uM) from MTS assay against each of the cells tested.

Table 4 lists 50% cytotoxic concentrations (CC_{50}), defined as the concentration at which there is a 50% reduction in cell viability as compared to an untreated control, for each of the peptides against each of the cells tested. For all the cells tested, CRAC motif containing peptides displayed similar cytotoxicity to WLBU2 with no statistically significant differences between CC_{50} values. In comparing CC_{50} for each peptide across the cell lines tested, there was no significant difference between cytotoxicity observed on transformed and non-transformed cell lines.

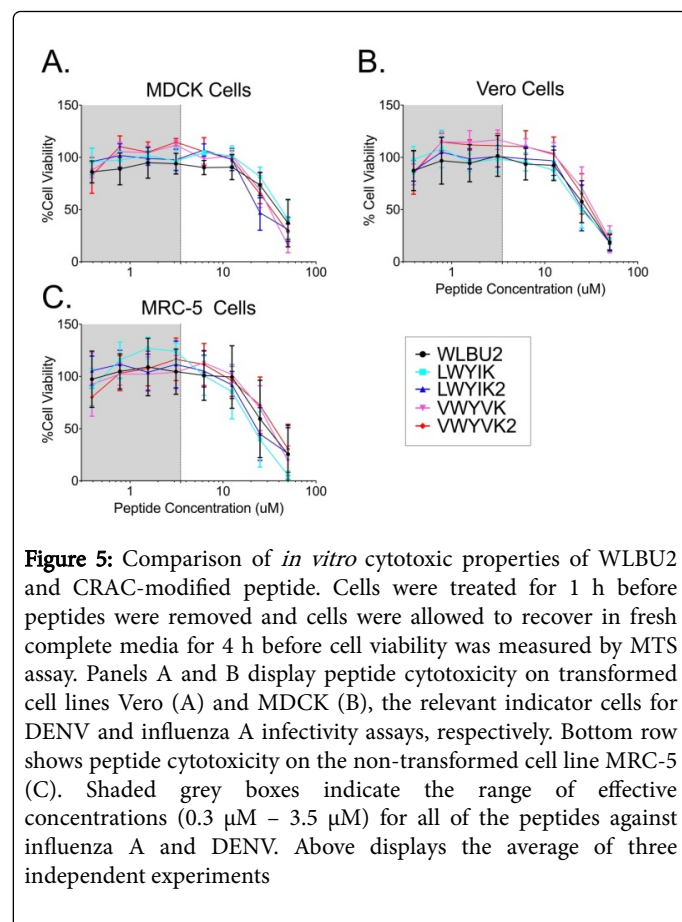


Figure 5: Comparison of *in vitro* cytotoxic properties of WLBU2 and CRAC-modified peptide. Cells were treated for 1 h before peptides were removed and cells were allowed to recover in fresh complete media for 4 h before cell viability was measured by MTS assay. Panels A and B display peptide cytotoxicity on transformed cell lines Vero (A) and MDCK (B), the relevant indicator cells for DENV and influenza A infectivity assays, respectively. Bottom row shows peptide cytotoxicity on the non-transformed cell line MRC-5 (C). Shaded grey boxes indicate the range of effective concentrations (0.3 uM – 3.5 uM) for all of the peptides against influenza A and DENV. Above displays the average of three independent experiments

Selective indices against influenza A and DENV

Selective indices for each of the peptides against influenza A and DENV listed in Table 5 were calculated using CC_{50} values calculated by MTS assay for MDCK cells and Vero cells, respectively. For influenza A, selective indices for CRAC motif containing peptides were about 2-fold greater than the selective index of WLBU2. In the case of LWYIK2, the selective index was 4-fold higher than the selective index for unmodified WLBU2 indicating that the peptide has similar cytotoxic affect, but with greater antiviral activity. For DENV, selective indices of CRAC motif containing peptides ranged from 52.5 to 188.3. VWYVK2 had the greatest selective index at 188.3, a 22-fold increase over unmodified WLBU2. Similarly, LWYIK2 had a selective index of 155.5, an 18-fold increase over WLBU2. The selective indices for DENV indicate that CRAC motif containing peptides have greater antiviral activity than unmodified WLBU2. There are currently no approved antiviral treatments for DENV infection to which selective indices could be compared.

Peptide	Influenza A	DENV
WLBU2	11.3	8.8
LWYIK	23.2	76.8
LWYIK2	45.4	155.5
VWYVK	14.6	52.8
VWYVK2	28.7	188.3

Table 5: Selective indices of peptides comparing CC_{50} of MDCK and Vero cells to EC_{50} against influenza A and DENV, respectively.

Characterization of peptide hemolytic and cytotoxic properties against human blood cells

To investigate the potential cytotoxic effects of peptides against primary human cells, hemolytic assays were carried out in whole blood and cell viability was measured for isolated PBMC. In the context of whole blood, peptides displayed no detectable hemolytic activity (data not shown). PBMC isolated from whole blood were treated with peptide for 1 h before cell viability was measured by flow cytometric analysis using a fixable live/dead stain. Treatments ranged from peptide concentrations of 25 μ M to 0.39 μ M (Figure 6). For all of the peptides tested, cytotoxicity was observed at 25 μ M, where the peptide VWYVK displayed the smallest reduction in viability of about 32%. As concentration of peptides decreased, cell viability increased, with little to no reduction of viability observed at concentrations less than or equal to 6.25 μ M for WLBU2 and LWYIK. These data indicate that VWYVK displays very little cytotoxicity on PBMC, while peptides containing two CRAC motifs are more cytotoxic, especially as compared at lower peptide concentrations.

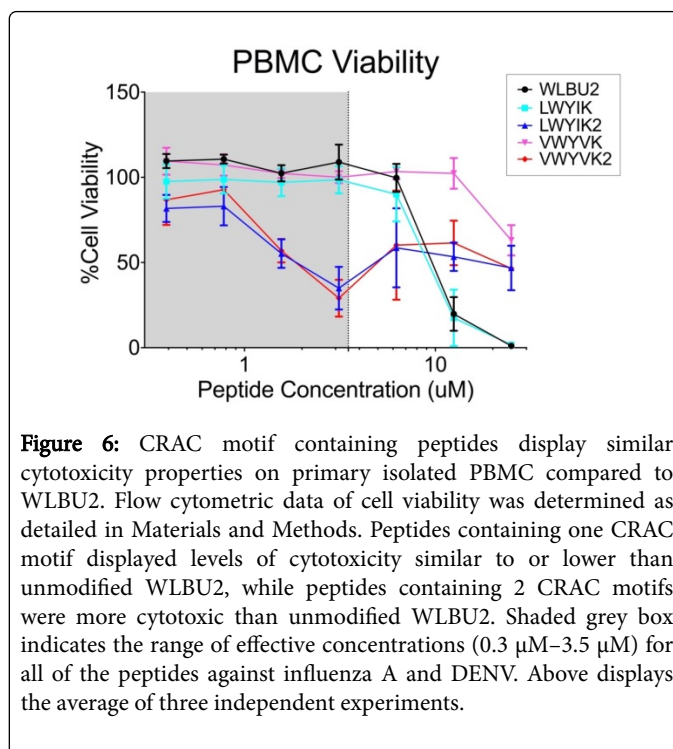


Figure 6: CRAC motif containing peptides display similar cytotoxicity properties on primary isolated PBMC compared to WLBU2. Flow cytometric data of cell viability was determined as detailed in Materials and Methods. Peptides containing one CRAC motif displayed levels of cytotoxicity similar to or lower than unmodified WLBU2, while peptides containing 2 CRAC motifs were more cytotoxic than unmodified WLBU2. Shaded grey box indicates the range of effective concentrations (0.3 μ M–3.5 μ M) for all of the peptides against influenza A and DENV. Above displays the average of three independent experiments.

Discussion

Antimicrobial peptides have emerged as promising candidates for antiviral treatments due to their potential for broad activity. Current research in cationic antiviral peptides has produced promising results, though no treatments have yet advanced to clinical studies [21]. Antimicrobial peptide development has been based on the use of natural AMPs and on the design of *de novo* engineered peptides with antiviral activity [69-72]. Previous studies have shown the potential for developing peptides with antiviral activity against viruses including HIV [73], influenza A [24], respiratory syncytial virus [74], DENV [75], and vaccinia virus [26]. The structural diversity of antimicrobial peptides is consistent with multiple mechanisms of action [76], including preventing fusion of the virus and cell membranes [77], blocking viral entry or replication [78], and modulating cellular antiviral responses [79]. One common mechanism of antiviral peptides is blocking viral entry by disrupting the envelope integrity and function, due to direct interactions between the peptide and the lipid bilayer [69,80-82]. The selectivity of these peptides relies on differences between the host cell and viral lipid membranes. Many viruses bud progeny virions from cholesterol-rich regions of membrane so that viral envelopes are markedly enriched for cholesterol as compared to the host cell membrane [32,35,36]. Designing eCAPs to interact with cholesterol-rich membranes could produce peptides with selective antiviral activity by directing them specifically to viral envelopes.

Here we report structure-function studies describing a novel viral envelope targeting strategy that was designed to take advantage of cholesterol-directing sequences to specifically target eCAPs to enveloped viruses for inactivation. The well-characterized eCAP, WLBU2, was modified to add cholesterol targeting CRAC sequences to the N-terminus either once or twice. We hypothesized that addition of cholesterol targeting sequences would create antiviral peptides that display activity based on viral lipid surface exposure, based on peptide

interactions with the viral envelope. When tested against HIV, influenza A, and DENV, we found that WLBU2 and CRAC motif containing peptides all displayed antiviral activity against influenza A virus and DENV, while enhancement of infectivity was observed with HIV. Thus, antiviral activity of CRAC motif containing peptides does not appear to be based on lipid surface exposure and, surprisingly, viruses with less lipid exposure were most sensitive to peptide treatment. These studies indicate the possibility of other mechanisms of inactivation and serve as a foundation for further mechanistic studies.

In order to determine the range of activity for cholesterol-targeting eCAPs, antiviral activity was assessed *in vitro* against a panel of viruses with varying levels of membrane protein content and surface lipid exposure. WLBU2 and the CRAC motif containing peptides all enhanced HIV infection *in vitro*, despite the high level of lipid exposure. The surface of the HIV virion is sparsely populated by Env proteins with a high lipid surface exposure, which allows peptide access to the membrane for disruption. Surprisingly however, peptide treatment of HIV led to enhancement of infection. The mechanism leading to this enhancement phenomenon is uncertain. Other groups have demonstrated that cationic amphipathic peptides can enhance lentiviral transduction efficiency. *In vivo*, the semen protein semen-derived enhancer of viral infection (SEVI) [83] has been shown to act as a polycationic bridge to neutralize repulsion effects between a negatively charged virion and target cell thereby leading to enhancement of infection [84]. Peptides that have been previously reported to display antiviral activity against HIV often block virus-cell interactions or block viral gene expression, such as by inhibiting integrase [85] or reverse transcriptase activity [86].

In marked contrast to HIV, WLBU2 and the CRAC motif containing peptides reduced infection by influenza A virus and DENV *in vitro*. In the case of influenza A, CRAC motif containing peptides performed similarly to WLBU2. Other antiviral peptides that have demonstrated activity against influenza A have displayed similar activity and EC₅₀ values [72,87,88]. For DENV, CRAC motif containing peptides had EC₅₀ values about 10- to 20-fold lower than unmodified WLBU2, with submicromolar EC₅₀ values. Other peptide inhibitors of flavivirus infection have reported EC₅₀ values 10- to 100-fold greater than those observed for CRAC motif peptides [89]. Contrary to the hypothesis under which these peptides were designed, DENV was the most sensitive to inactivation by eCAPs in virus pretreatment assays. This observation suggests that there may be other mechanisms of virus inactivation in addition to the predicted lipid disruption. In order to explore this further, VeroE6 cells were pretreated with peptides before infection with DENV to determine whether peptide presence during infection is necessary for antiviral activity. When CRAC motif containing peptides were removed before infection with DENV, significantly decreased antiviral activity was observed, indicating that peptide must be present during infection to maintain antiviral activity. While CRAC motif containing peptides were designed to interact directly with virion lipids, peptides may exert antiviral activity when present during infection by direct interaction with host factors such as cellular receptors for infection. The cellular receptors of influenza A and DENV, sialic acid [90] and heparan sulfate [91], respectively, are both negatively charged glycoproteins found on the cell surface. Because these eCAP peptides are highly cationic, introduction of these peptides during infection may block viral entry by peptide binding to cell surface receptors, thus blocking interactions between viruses and their necessary receptors. Other engineered cationic peptides have demonstrated that HSV entry can be

blocked by peptide interaction with heparan sulfate [92], indicating a similar mechanism could be at play with CRAC motif containing peptides. Further temporal and mechanistic studies are necessary, including confocal microscopy studies using fluorescently tagged peptides to see whether peptides colocalize with necessary receptors for viral entry.

In order to determine whether CRAC motif containing peptides are cytotoxic on relevant cells at the concentrations at which antiviral activity is demonstrated, we measured the cytotoxic effect of our peptides using three standard methods to analyze a panel of primary, transformed, and non-transformed cells: red blood cell lysis, flow cytometry, and MTS assay. As measured by all three assays, the lowest effective antiviral concentrations of peptide do not significantly alter host cell viability. In the context of whole blood, none of the peptides displayed significant hemolysis at any of the concentrations of peptide tested. As measured by flow cytometric analysis, cytotoxicity greater than 50% was only observed at peptide treatments at least 4-times as great as peptide effective concentrations. Similarly, MTS assays indicate cytotoxicity greater than 50% was only observed at peptide concentrations at least 10-fold greater than peptide effective concentrations. While these initial studies indicate limited cytotoxicity at the effective concentrations of peptide, it is difficult to correlate these *in vitro* data to *in vivo* activity. The prophylactic or therapeutic use *in vivo* of these CRAC motif containing peptides will depend on many different factors including formulation, bioavailability, and biodistribution. Pharmacokinetic and pharmacodynamic studies are also warranted in order to consider peptides for therapeutic potential.

Based on the antiviral activity and cytotoxicity data, both the LWYIK and VWYVK CRAC motifs behave similarly to one another. This indicates that CRAC motifs can be designed synthetically with similar levels of activity to naturally occurring sequences. The results also indicate that there is no additive effect with addition of multiple CRAC motifs in the context of short peptide sequences. Overall, these data have important implications in eCAP design. The pattern of antiviral activity observed with these peptides against the chosen panel of viruses indicates that the mechanism of action of these eCAPs against mammalian viruses may not be exclusively or predominantly dependent on lipid exposure as previously presumed. Our results indicate that viruses with less lipid surface exposure may be more susceptible to peptide treatment and that peptide must be present during infection for optimum antiviral effect. This suggests that there is a different mechanism of antiviral activity for these peptides possibly requiring peptide-host interactions. While the results presented here strongly suggest a distinctive mechanism of action, these deductions are indirectly derived. Additional studies are required for a more thorough analysis of potential mechanism of action. Establishing what this mechanism is will be important in developing peptides with enhanced antiviral activity, determining other virus species against which these peptides would be effective, and discovering possible viral resistance strategies.

Acknowledgements

This study is funded by discretionary funds from the Center for Vaccine Research (<http://www.cvr.pitt.edu/>). The authors would like to thank Dr. Kelly Stefano-Cole for generously supplying influenza A virus strain PR8 and MDCK cells. The authors would also like to extend thanks to Dr. Ernesto Marques for allowing use of DENV2 stocks and providing Vero cells. R.C.M., J.D.S., and J.K.C. hold stock in Peptilogics, Inc. R.C.M. serves on an advisory board for Peptilogics,

and J.D.S. has a management role at Peptilogics. Although a potential financial conflict of interest was identified based on the authors' relationship with Peptilogics, the research findings included in this publication may not necessarily be related to the interests of Peptilogics.

References

1. De Clercq E (2004) Antivirals and antiviral strategies. *Nat Rev Microbiol* 2:704-720.
2. Javadpour MM, Juban MM, Lo W-CJ, Bishop SM, Alberty JB, et al. (1996) De novo antimicrobial peptides with low mammalian cell toxicity. *J Med Chem* 39: 3107-3113.
3. Tew GN, Liu D, Chen B, Doerksen RJ, Kaplan J, et al. (2002) De novo design of biomimetic antimicrobial polymers. *Proc Natl Acad Sci USA* 99: 5110-5114.
4. Friedrich C, Scott MG, Karunaratne N, Yan H, Hancock REW (1999) Salt-resistant alpha-helical cationic antimicrobial peptides. *Antimicrob Agents Chemother* 43: 1542-1548.
5. Braff MH, Gallo RL (2006) Antimicrobial peptides: an essential component of the skin defensive barrier. *Curr Top Microbiol Immunol* 306: 91-110.
6. Hancock REW, Scott MG (2000) The role of antimicrobial peptides in animal defenses. *Proc Natl Acad Sci USA* 97: 8856-8861.
7. Eband RM, Vogel HJ (1999) Diversity of antimicrobial peptides and their mechanisms of action. *Biochim Biophys Acta* 1462: 11-28.
8. Zasloff M (2002) Antimicrobial peptides of multicellular organisms. *Nature* 415: 389-395.
9. Peters BM, Shirliff ME, Jabra-Rizk MA (2010) Antimicrobial peptides: primeval molecules or future drugs? *PLoS Pathog* 28: e1001067.
10. Hancock REW, Sahl HG (2006) Antimicrobial and host-defense peptides as new anti-infective therapeutic strategies. *Nat Biotechnol* 24: 1551-1557.
11. Melo MN, Castanho MARB (2012) The mechanism of action of antimicrobial peptides: lipid vesicles vs. bacteria. *Front Immunol* 3.
12. Nissen-Meyer J, Nes IF (1997) Ribosomally synthesized antimicrobial peptides: their function, structure, biogenesis, and mechanism of action. *Arch Microbiol* 167: 67-77.
13. Shai Y, Oren Z (2001) From "carpet" mechanism to de-novo designed diastereomeric cell-selective antimicrobial peptides. *Peptides* 22: 1629-1641.
14. Haney EF, Nguyen LT, Schibli DJ, Vogel HJ (2012) Design of a novel tryptophan-rich membrane-active antimicrobial peptide from the membrane-proximal region of the HIV glycoprotein, gp41. *Beilstein J Org Chem* 8: 1172-1184.
15. Chen Y, Mant CT, Farmer SW, Hancock REW, Vasil ML, et al. (2005) Rational design of α -helical antimicrobial peptides with enhanced activities and specificity/therapeutic index. *J Biol Chem* 280: 12316-12329.
16. Deslouches B, Islam K, Craig JK, Paranjape SM, Montelaro RC, et al. (2005) Activity of the de novo engineered antimicrobial peptide WLBU2 against *Pseudomonas aeruginosa* in human serum and whole blood: implications for systemic applications. *Antimicrob Agents Chemother* 49: 3208-3216.
17. Deslouches B, Phadke SM, Lazarevic V, Cascio M, Islam K, et al. (2005) De novo generation of cationic antimicrobial peptides: influence of length and tryptophan substitution on antimicrobial activity. *Antimicrob Agents Chemother* 49: 316-322.
18. Deslouches B, Steckbeck JD, Craig JK, Doi Y, Mietzner TA, et al. (2013) Rational design of engineered cationic antimicrobial peptides consisting exclusively of arginine and tryptophan, and their activity against multidrug-resistant pathogens. *Antimicrob Agents Chemother* 57: 2511-2521.
19. Deslouches B, Gonzalez IA, DeAlmeida D, Islam K, Steele C, et al. (2007) De novo-derived cationic antimicrobial peptide activity in a murine model of *Pseudomonas aeruginosa* bacteraemia. *J Antimicrob Chemother* 60: 669-672.
20. Carriel-Gomes MC, Kratz JM, Barracco MA, Bachere IV E, Baradi CRM, et al. (2007) In vitro antiviral activity of antimicrobial peptides against herpes simplex virus 1, adenovirus, and rotavirus. *Mem Inst Oswaldo Cruz* 102: 469-472.
21. Mulder KC, Lima LA, Miranda VJ, Dias SC, Franco OLF, et al. (2013) Current scenario of peptide-based drugs: the key roles of cationic antitumor and antiviral peptides. *Front Microb* 4: 321.
22. Yasin B, Wang W, Pang M, Cheshenko N, Hong T, et al. (2004) fensins protect cells from infection by herpes simplex virus by inhibiting viral adhesion and entry. *J Virol* 78: 5147-5156.
23. Berkhout B, Floris R, Recio I, Visser S (2004) The antiviral activity of the milk protein lactoferrin against the human immunodeficiency virus type 1. *Biomaterials* 17: 291-294.
24. Tripathi S, Teclé T, Verma A, Crouch E, White MR. (2013) The human cathelicidin LL-37 inhibits influenza A viruses through a mechanism distinct from that of surfactant protein D or defensins. *J Gen Virol* 94: 40-49.
25. Bergman P, Walter-Jallow L, Broliden K, Agerberth B, Soderlund J (2007) The antimicrobial peptide LL-37 inhibits HIV-1 replication. *Curr HIV Res* 5: 410-415.
26. Howell MD, Jones JF, Kisich KO, Streib JE, Gallo RL, et al. (2004) Selective killing of vaccinia virus by LL-37: implications for eczema vaccinatum. *J Immunol* 172: 1763-1767.
27. Isaacs CE, Rohan L, Xu W, Jia JH, Mietzner T, et al. (2006) Inactivation of herpes simplex virus clinical isolates by using a combination microbicide. *Antimicrob Agents Chemother* 50: 1063-1066.
28. Colpitts CC, Ustinov AV, Eband RF, Eband RM, Korshun VA, et al. (2013) 5-(Perylen-3-yl) Ethynyl-arabino-uridine (aUY11), an arabino-based rigid amphipathic fusion inhibitor, targets virion envelope lipids to inhibit fusion of influenza virus, hepatitis C virus, and other enveloped viruses. *J Virol* 87: 3640-3654.
29. Lenard J (1978) Virus envelopes and plasma membranes. *Ann Rev Biophys Bioeng* 7: 139-165.
30. Chazal N, Gerlier D (2003) Virus entry, assembly, budding, and membrane rafts. *Microbiol Mol Biol Rev* 67: 226-237.
31. Spector AA, Kiser RE, Denning GM, Koh S, DeBault LE (1979) Modification of the fatty acid composition of cultured human fibroblasts. *J Lipid Res* 20: 536-547.
32. Aloia RC, Tian H, Jensen FC (1993) Lipid composition and fluidity of the human immunodeficiency virus envelope and host cell plasma membranes. *Proc Natl Acad Sci USA* 90: 5181-5185.
33. Cordero JG, Juarez ML, Gonzalez-Y-Merchand JA, Barron LC, et al. (2014) Caveolin-1 in lipid rafts interacts with dengue virus NS3 during polyprotein processing and replication in HMEC-1 cells. *Plos one*.
34. Scheiffele P, Rietveld A, Welk T, Simons K (1999) Influenza viruses select ordered lipid domains during budding from the plasma membrane. *J Biol Chem* 274: 2038-2044.
35. Sun X, Whittaker GR (2003) Role for influenza virus envelope cholesterol in virus entry and infection. *J Virol* 77: 12543-12551.
36. Carro AC, Damonte EB (2013) Requirement of cholesterol in the viral envelope for dengue virus infection. *Virus Res* 174: 78-87.
37. Brugger B, Glass B, Haberkant P, Leibrecht I, Wieland FT, et al. (2005) The HIV lipidome: a raft with unusual composition. *Proc Natl Acad Sci USA* 103: 2641-2646.
38. Li H, Papadopoulos V (1998) Peripheral-type benzodiazepine receptor function in cholesterol transport. Identification of a putative cholesterol recognition/interaction amino acid sequence and consensus pattern. *Endocrinology* 139: 4991-4997.
39. Eband RM (2006) Cholesterol and the interaction of proteins with membrane domains. *Prog Lipid Res* 45: 279-294.
40. Vishwanathan SA, Thomas A, Brasseur R, Eband RF, Hunter E, et al. (2008) Large changes in the CRAC segment of the gp41 of HIV does not

- destroy fusion activity if the segment interacts with cholesterol. *Biochemistry* 47: 11869-11876.
41. Chertova E, Bess Jr JW, Crise BJ, Sowder II RC, Schaden TM, et al. (2002) Envelope glycoprotein incorporation, not shedding of surface envelope glycoprotein (gp120/SU), is the primary determinant of SU content of purified human immunodeficiency virus type 1 and simian immunodeficiency virus. *J Virol* 76: 5315-5325.
 42. Nguyen DH, Hildreth JEK (2000) Evidence for budding of human immunodeficiency virus type 1 selectivity from glycolipid-enriched membrane lipid rafts. *J Virol* 74: 3264-3272.
 43. Medina RA, Garcia-Sastre A (2011) Influenza A viruses: new research developments. *Nat Rev Microbiol* 9: 590-603.
 44. Harris AK, Meyerson JR, Matsuoka Y, Kuybeda O, Moran A, et al. (2013) Structure and accessibility of HA trimers on intact 2009 H1N1 pandemic influenza virus to stem region-specific neutralizing antibodies. *PNAS* 110: 4592-4597.
 45. Kuhn RJ, Zhang W, Rossmann MG, Pletnev SV, Corver J, et al. (2002) Structure of dengue virus: implications for flavivirus organization, maturation, and fusion. *Cell* 108: 717-725.
 46. Modis Y, Ogata S, Clements D, Harrison SC (2004) Structure of the dengue virus envelope protein after membrane fusion. *Nature* 427.
 47. Perera R, Kuhn RJ (2008) Structural proteomics of dengue virus. *Curr Opin Microbiol* 11: 369-377.
 48. Maupetit J, Tuffery P, Derreumaux P (2007) A coarse-grained protein force field for folding and structure prediction. *Proteins* 69: 394-408.
 49. Thevenet P, Shen Y, Maupetit M, Guyon F, Derreumaux P, et al. (2012) PEP-FOLD: an updated de novo structure prediction server for both linear and disulfide bonded cyclic peptides. *Nucleic Acids Res* 40: 288-293.
 50. Gautier R, Douguet D, Antony B, Drin G (2008) HELIQUEST: a web server to screen sequences with specific α -helical properties. *Bioinformatics* 24: 2101-2102.
 51. Fontenot JD, Ball JM, Miller MA, David CM, Montelaro RC (1991) A survey of potential problems and quality control in peptide synthesis by the fluorenylmethoxycarbonyl procedure. *Pept Res* 4: 19-25.
 52. Whitmore L, Wallace BA (2007) Protein secondary structure analyses from circular dichroism spectroscopy: methods and reference databases. *Biopolymers* 89: 392-400.
 53. Compton LA, Johnson Jr C (1986) Analysis of protein circular dichroism spectra for secondary structure using a simple matrix multiplication. *Anal Biochem* 155: 155-167.
 54. Manavalan P, Johnson Jr C (1987) Variable selection method improves the prediction of protein secondary structure from circular dichroism spectra. *Anal Biochem* 167: 76-85.
 55. Sreerama N, Woody RW (2000) Estimation of protein secondary structure from circular dichroism spectra: comparison of CONTIN, SELCON, and CDSSTR methods with an expanded reference set. *Anal Biochem* 287: 252-260.
 56. Lees JG, Miles AJ, Wien F, Wallace BA (2006) A reference database for circular dichroism spectroscopy covering fold and secondary structure space. *Bioinformatics* 22: 1955-1962.
 57. Montefiori DC (2009) Measuring HIV neutralization in a luciferase reporter gene assay. *Methods Mol Biol* 485: 395-405.
 58. Gaush CR, Smith TF (1968) Replication and plaque assay of influenza virus in an established line of canine kidney cells. *Appl Microbiol* 16: 588-594.
 59. Russell PK, Nisalak A, Sukhavachana P, Vivona S (1967) A plaque reduction test for dengue virus neutralizing antibodies. *J Immunol* 99: 285-290.
 60. Cory AH, Owen TC, Barltrop JA, Cory JG (1991) Use of an aqueous soluble tetrazolium/formazan assay for cell growth assays in culture. *Cancer Commun* 3:207-212.
 61. Berridge MV, Herst PM, Tan AS (2005) Tetrazolium dyes as tools in cell biology: new insights in their cellular reduction. *Biotechnol Annu Rev* 11: 127-152.
 62. Mosmann T (1983) Rapid colorimetric assay for cellular growth and survival: application to proliferation and cytotoxicity assays. *J Immunol Methods* 65: 55-63.
 63. Apellaniz B, Ivankin A, Nir S, Gidalevitz D, Nieva JL (2011) Membrane-proximal external HIV-1 gp41 motif adapted for destabilizing the highly rigid viral envelope. *Biophys J* 101: 2426-2435.
 64. Ivankin A, Apellaniz B, Gidalevitz D, Nieva JL (2012) Mechanism of membrane perturbation by the HIV-1 gp41 membrane-proximal external region and its modulation by cholesterol. *Biochim Biophys Acta* 1818: 2521-2528.
 65. Kelly SM, Jess TJ, Price NC (2005) How to study proteins by circular dichroism. *Biochim Biophys Acta* 1751.
 66. Tiffany JM, Blough HA (1970) Models of structure of the envelope of influenza virus. *Proc Natl Acad Sci USA* 65: 1105-1112.
 67. Liu J, Shi X, Schwartz R, Kemble G (2009) Use of MDCK cells for production of live attenuated influenza vaccine. *Vaccine* 27: 6460-6463.
 68. Chang CW, Chen CR, Huang CY, Shu WY, Chiang CS, et al. (2013) Comparative transcriptome profiling of an SV40-transformed human fibroblast (MRC5CVI) and its untransformed counterpart (MRC-5) in response to UVB irradiation. *Plos one*.
 69. Daher KA, Selsted ME, Lehrer R (1986) Direct inactivation of viruses by human granulocyte defensins. *J Virol* 60.
 70. Costin JM, Jenwitheesuk E, Lok S-M, Hunsperger E, Conrads KA, et al. (2010) Structural optimization and de novo design of dengue virus entry inhibitory peptides. *PLoS Negl Trop Dis* 4.
 71. Wang G, Buckheit KW, Mishra B, Lushnikova T, Buckheit Jr RW (2011) De novo design of antiviral and antibacterial peptides with varying loop structures. *J AIDS Clinic Res* S2.
 72. Tripathi S, Wang G, White MR, Qi L, Taubenberger J, et al. (2015) Antiviral activity of the human cathelicidin LL-37, and derived peptides on seasonal and pandemic influenza A viruses. *Plos one*.
 73. Zhang H, Curreli F, Zhang X, Bhattacharya S, Waheed AA, et al. (2011) Antiviral activity of α -helical stapled peptides designed from the HIV-1 capsid dimerization domain. *Retrovirology* 8.
 74. Currie SM, Findlay EG, McHugh BJ, Mackellar A, Man T, et al. (2013) The human cathelicidin LL-37 has antiviral activity against respiratory syncytial virus. *PLoS One* 8: e73659.
 75. Schmidt AG, Yang PL, Harrison SC (2010) Peptide inhibitors of flavivirus entry derived from the E protein stem. *J Virol* 84.
 76. Jensen H, Hamill P, Hancock REW (2006) Peptide Antimicrobial Agents. *Clinical Microbiology Reviews* 19.
 77. Wolf MC, Freiberg AN, Zhang T, Akyol-Ataman Z, Grock A, et al. (2010) A broad-spectrum antiviral targeting entry of enveloped viruses. *PNAS* 107.
 78. Wachinger M, Kleinschmidt A, Winder D, von Pechmann N, Ludvigsen A, et al. (1998) Antimicrobial peptides melittin and cecropin inhibit replication of human immunodeficiency virus 1 by suppressing viral gene expression. *J Gen Virol* 79.
 79. Wilson SS, Wiens ME, Smith JG (2013) Antiviral mechanisms of human defensins. *J Mol Biol* 425.
 80. Murakami T, Niwa M, Tokunaga F, Miyata T, Iwanaga S (1991) Direct virus inactivation of tachyplesin I and its isopeptides from horseshoe crab hemocytes. *Chemotherapy* 37.
 81. VanCompernelle SE, Taylor RJ, Oswald-Richter K, Jiang J, Youree BE, et al. (2005) Antimicrobial peptides from amphibian skin potentially inhibit human immunodeficiency virus infection and transfer of virus from dendritic cells to T cells. *J Virol* 79.
 82. Kota S, Sabbah A, Chang TH, Harnack R, Xiang Y, et al. (2008) Role of human α -defensin-2 during tumor necrosis factor- α /NF- κ B-mediated innate antiviral response against human respiratory syncytial virus. *J Biol Chem* 283.
 83. Munch J, Rucker E, Stanker L, Adermann K, Goffinet C, et al. (2007) Semen-derived amyloid fibrils drastically enhance HIV infection. *Cell* 131: 1059-1071.

84. Roan NR, Munch J, Arhel N, Mothes W, Neideman J, et al. (2008) The cationic properties of SEVI underlie its ability to enhance human immunodeficiency virus infection. *J Virol* 83: 73-80.
85. Krajewski K, Marchand C, Long YQ, Pommier Y, Roller PP (2004) Synthesis and HIV-1 integrase inhibitory activity of dimeric and tetrameric analogs of indolicidin. *Bioorg Med Chem Lett* 14: 5595-5598.
86. Wong JH, Legowska A, Rolka K, Ng Tb, Hui M, et al. (2011) Effects of cathelicidin and its fragments on three key enzymes of HIV-1. *Peptides* 32: 1117-1122.
87. Jones JC, Turpin EA, Bultmann H, Brandt CR, Schultz-Cherry S (2006) Inhibition of influenza virus infection by a novel antiviral peptide that targets viral attachment to cells. *J Virol* 80.
88. Salvatore M, Garcia-Sastre A, Ruchala P, Lehrer R, Chang T, et al. (2007) alpha-defensin inhibits influenza virus replication by cell mediated mechanism(s). *J Infect Dis* 196: 835-843.
89. Alhoot MA, Rathinam AK, Wang SM, Manikam R, Sekaran SD (2013) Inhibition of dengue virus entry into target cells using synthetic antiviral peptides. *Inter J of Med Sci* 10.
90. Nicholls JM, Chan RWY, Russell RJ, Air GM, Peiris M (2008) Evolving complexities of influenza virus and its receptors. *Trends Microbiol* 16: 149-157.
91. Roehrig JT, Butrapet S, Liss NM, Bennett SL, Luy BE, et al. (2013) Mutation of the dengue virus type 2 envelope protein heparan sulfate binding sites or the domain III lateral ridge blocks replication in Vero cells prior to membrane fusion. *Virology* 441: 114-125.
92. Anderson JH, Jenssen H, Sandvik K, Gutteberg TJ (2004) Anti-HSV activity of lactoferrin and lactoferricin is dependent on the presence of heparan sulphate at the cell surface. *J Med Virol* 74.